CORRELATION BETWEEN MICROSTRUCTURE AND EXCHANGE COUPLING PARAMETERS OF Ir-Mn BASED MTJ

T. STOBIECKI[1], J. KANAK[1], J. WRONA[1], M. CZAPKIEWICZ[1], C. G. KIM[2], C. O. KIM[2], M. TSUNODA[3] AND M. TAKAHASHI[3]

[1]*Department of Electronics, AGH University of Science and Technology*
Al. Mickiewicza 30, 30-059 Krakow, Poland

[2]*Department of Materials Engineering, Chungnam National University, 305-764 Daejon, Korea*

[3]*Department of Electronic Engineering, Tohoku University, 980-8579 Sendai, Japan*

Abstract: Magnetic tunnel junctions (MTJs) with the structure Si(100)/Si-O$_x$//Ta(5)/Cu(10)/Ta(5)-/NiFe(2)/Cu(5)/IrMn(10)/CoFe(2.5)/Al-O/CoFe(2.5)/NiFe(t)/Ta(5), where t = 10, 30, 60 and 100 nm in as-deposited and annealed state were characterized by XRD and magnetic hysteresis loop measurements. The XRD measurements were done in grazing incidence (GID scan-2θ) and θ-2θ geometry, by rocking curve (scan-ω) and pole figures in order to establish correlation between microstructure (texture and crystallites size) and magnetic parameters of exchange biased and interlayer coupling. Annealing in vacuum at 300°C led to an increase of average crystallite size of Ir$_{25}$Mn$_{75}$ and Ni$_{80}$Fe$_{20}$ and improvement of (111) plane-texture of Ir$_{25}$Mn$_{75}$, Cu and Ni$_{80}$Fe$_{20}$. The exchange biased fields and the coercivity of the pinned layer linearly increased with increasing grain size of IrMn. The reciprocal proportionality between interlayer coupling field and coercivity of the free layer and grain size of NiFe was found. The enhancement of interlayer coupling between pinned and free layers, after annealing treatment, indicates the correlated in-phase roughness of dipolar interacting interfaces due to increase of crystallites size of NiFe.

1. INTRODUCTION

For read head and M-RAM cells applications, spin valve or magnetic tunnel junction (MTJ) films with: large exchange biased field (H_{EB}), high magnetoresistance (MR) or tunnel magnetoresistance (TMR), high blocking temperature, and thin free layers are required. Compared to other antiferromagnets (AF) like FeMn, NiO, CrMnPt, and PtMn [1], IrMn has been found as very promising AF material due to its high exchange bias energy ($J_{EB} \approx 4 \cdot 10^{-4}$J/m^2), high blocking temperature ($T_b \approx 590$ K) and low critical thickness (~7 nm) [2]. The exchange coupling between (AF) /ferromagnetic (F) layers, which has been shown primarily to be an interfacial phenomenon [3], should be dependent on the microstructural characteristics of the films such as crystal texture, grain size and roughness. All these factors influence on the interface microstructure and are closely linked to the structure of the growth/buffer and underlayers which are used in designed junctions [4, 5]. The large exchange bias field values reported in the literature [5-8] are associated with an increase of the (111)-*fcc* texture and grain size obtained after annealing [9, 10], but some contrary opinions have been given in the literature either [11].

In this work we discuss diffraction measurements, carried out very precisely and systematically, for as deposited and annealed junctions with the structure of Ta(5)/Cu(10)/Ta(5)-/NiFe(2)/Cu(5)/IrMn(10)/CoFe(2.5)/Al-0/CoFe(2.5)/NiFe(t)/Ta(5) where t = 10, 30, 60 and 100 nm, in order to establish correlation between structure ((111)-*fcc* texture and grain size of Cu, $Ir_{25}Mn_{75}$ and $Ni_{80}Fe_{20}$ sublayers of the stack) and magnetic parameters of interfacial and interlayer exchange coupling. The determination of the grain size of NiFe-free layer, using grazing incidence diffraction (GID), allowed to find reciprocal proportionality between interlayer field (H_S) and grain size of NiFe. Bearing in mind potential applications, the thickness of free layer of MTJ should be as thin as possible, however XRD measurements are sufficiently accurate for thickness as greater than 10 nm.

2. EXPERIMENT

The tunnel junctions with the structure given above were prepared, in laboratory of Prof. M. Takahashi Tohoku University, on thermally oxidized Si wafers using DC magnetron sputtering with ultra clean Ar(9N) as the process gas, in a chamber with base pressure of 4×10^{-9} hPa. The barrier formation was performed by deposition of the 1.5 nm thick metallic Al film and subsequently oxidizing it in the oxidization chamber having a radial line slot antenna (RLSA) for 2.45 GHz-microwave. The details of this plasma oxidization technique are explained elsewhere [12]. The composition of antiferromagnetic layer $Ir_{25}Mn_{75}$ as well as the pinned layer $Co_{70}Fe_{30}$ are optimised to find the maximum value of the unidirectional anisotropy for the bottom type Ir-Mn/Co-Fe spin valve structure (see details in [14]). The samples were annealed in vacuum (10^{-6} hPa) under a magnetic field of 80 kA/m, followed by field cooling. These are optimum annealing conditions to obtain maximum of tunnelling MR ratio [13]. The magnetic measurements were performed by R-VSM and MOKE magnetometers described elsewhere [15]. In order to find the correlation between structure parameters and magnetic properties, the samples have been characterized by XRD experiment, using Philips diffractometer type X'Pert–MPD with Cu-anode, in GID (scan-2θ) and θ-2θ geometry and by rocking curve (scan-ω).

3. RESULTS AND DISCUSSION

3.1. Structure

Figure 1a shows specular XRD-profiles measured in wide range of diffraction angle 2θ for a series of as deposited MTJs with different free layer thickness. Except of Si-substrate peaks, β-Ta (002) and strong *fcc* textured peaks of $Ir_{25}Mn_{75}$ and Cu are observed (Fig. 1b). The lattice spacings determined from peak positions are: 0.2656 nm for Ta, 0.2180 nm for $Ir_{25}Mn_{75}$, 0.209 nm for Cu and 0.205 for $Ni_{80}Fe_{20}$. The comparison of θ-2θ and GID profiles for the as-deposited and annealed samples is presented in Fig. 2. Due to very close lattice planes of (111)Cu and (111)NiFe, GID measurement (under α = 5°) allowed the separation of Cu and NiFe peaks. The crystallite size of (111)$Ir_{25}Mn_{75}$, (111) Cu from θ-2θ-scans, and (111) $Ni_{80}Fe_{20}$ from GID-scans were determined, using high purity powder standard for calibration and program *Line Profile Analysis (LPA)*. In order to check the (111)-*fcc* planes orientation,
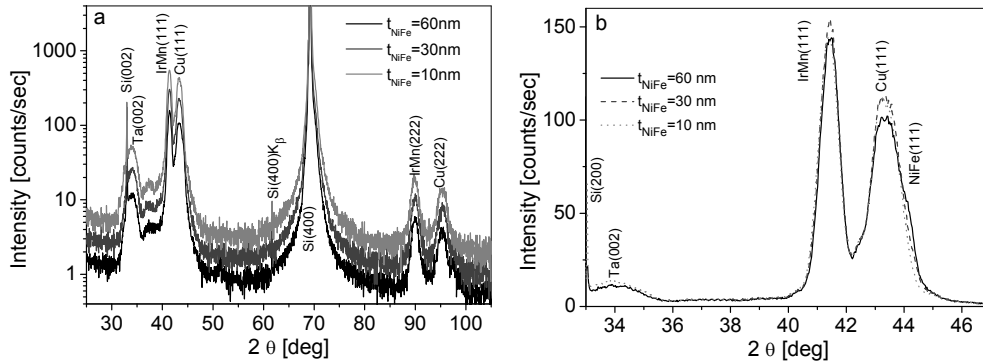
Fig. 1. XRD θ-2θ profiles for as-deposited MTJ (t = 10, 30, 60 nm), (a) wide range of diffraction angle 2θ where first and second order peaks of Cu and IrMn are observed (b) narrow range of 2θ
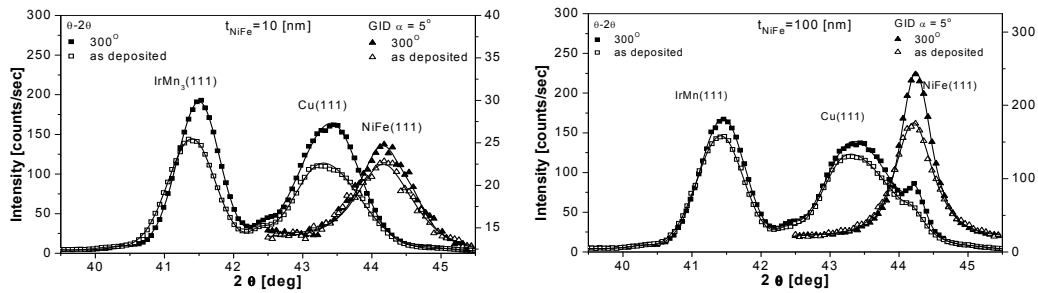

Fig. 2. θ-2θ and 2θ-GID scans for as-deposited and annealed MTJ (t = 10 and 100 nm) with fitting lines of *fcc*-(111)IrMn, (111)Cu and (111)NiFe peaks
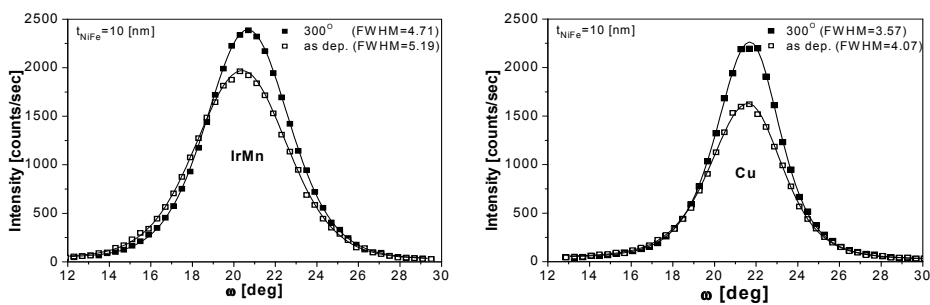

Fig. 3 Example rocking curves ω-scans for as-deposited and annealed MTJ (t = 10 nm) with fitting lines of *fcc*-(111)IrMn and (111)Cu

which is supposed to be in parallel to the surface of the substrate, rocking curves of these samples have been recorded. Typical rocking curves of IrMn(111) and Cu(111), for sample

with $t = 10$ nm, are shown in Fig. 3. The rocking curve peaks are symmetrical and centred at Bragg positions of IrMn(111) and Cu(111). The annealing treatment in vacuum at 300°C for 1 hour, causes an increase in (111) peak intensity and crystallites size of IrMn, Cu and NiFe. The lattice constants and FWHM (Full Width Half Maximum) of the IrMn(111), and Cu(111)-rocking curve peaks decrease, indicating an improvement in (111)-texture of multilayer structure (compare the changes of these parameters between as deposited and annealed samples collected in Table 1). Similar behaviour has been observed also for NiFe free layer where the lattice constants decrease and grain sizes increase after annealing (see Table 2).

Table 1. Structure parameters of $Ir_{25}Mn_{75}$ and Cu where t, a, D are given in nm and FWHM in angle degrees

MTJ	IrMn						Cu					
	as-deposited			annealed 300°C			as-deposited			annealed 300°C		
t	a	D	FWHM	a	D	FWHM	a	D	FWHM	a	D	FWHM
10	0.3776	7.0	5.19	0.3767	8.7	4.71	0.3618	4.7	4.07	0.3608	5.3	3.57
30	0.3772	7.5	5.04	0.3769	7.9	4.78	0.3614	4.2	3.88	0.3613	4.5	3.74
60	0.3771	7.7	4.95	0.3768	8.3	4.59	0.3616	4.0	3.90	0.3615	4.1	3.71
100	0.3774	7.1	5.13	0.3771	7.7	4.86	0.3619	4.5	3.83	0.3614	4.5	3.67

Table 2 Structure and magnetic parameters of NiFe, where H_S and H_{CF} are given in A/m

MTJ	NiFe							
	as-deposited				annealed 300°C			
t	a	D	H_S	H_{CF}	a	D	H_S	H_{CF}
10	0.3553	7.8	760	943	0.3553	10.1	935	764
30	0.3552	10.5	168	527	0.3548	14.3	465	282
60	0.3549	11.4	139	397	0.3547	31.7	192	177
100	0.3548	14.3	60	306	0.3545	41.7	149	243

The typical pole figures of *fcc*-IrMn, -Cu and -NiFe for as deposited and annealed samples (Fig. 4) depict centred [111] spots and spread rings around the angle $\psi = 70°$. Due to the increase of crystallites size, narrower and stronger intensity rings for annealed samples are observed. The (111) planes of IrMn and Cu are parallel to the substrate surface, which means that the sample has a (111) sheet texture with no crystallographic orientation in the film plane. The pole figure of NiFe (accurately measured only for NiFe thicker than 30 nm) represent wide spot [111] and weak diffuse ring in as deposited samples which means that NiFe crystallites are disoriented from [111] direction. After annealing the intensity of the central
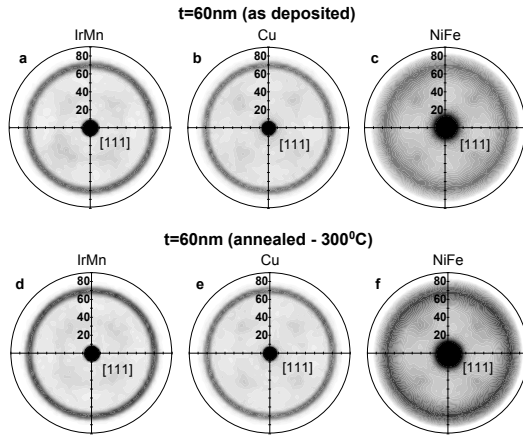
t=60nm (as deposited)

t=60nm (annealed - 300⁰C)

Fig. 4. Exemple pole figures of MTJ (t = 60 nm) for as-deposited: (a) IrMn{111}, (b) Cu{111}; (c) NiFe {111} and annealed: (d) IrMn{111} (e) Cu{111}, (f) NiFe {111}

spot and ring around the angle ψ = 70° increases while FWHM decreases. These changes lead to the improvement of the (111) plane texture of NiFe.

3.2. Interfacial exchange coupling

Figures 5a and 5c show the magnetization and TMR hysteresis loops for as deposited junction. Although the biased loop of ferromagnetic pinned (FP) layer is not observed in as-deposited junctions, thermal annealing, close to the blocking temperature and followed by magnetic field cooling, results in the shifted hysteresis loop of the FP layer, as shown in
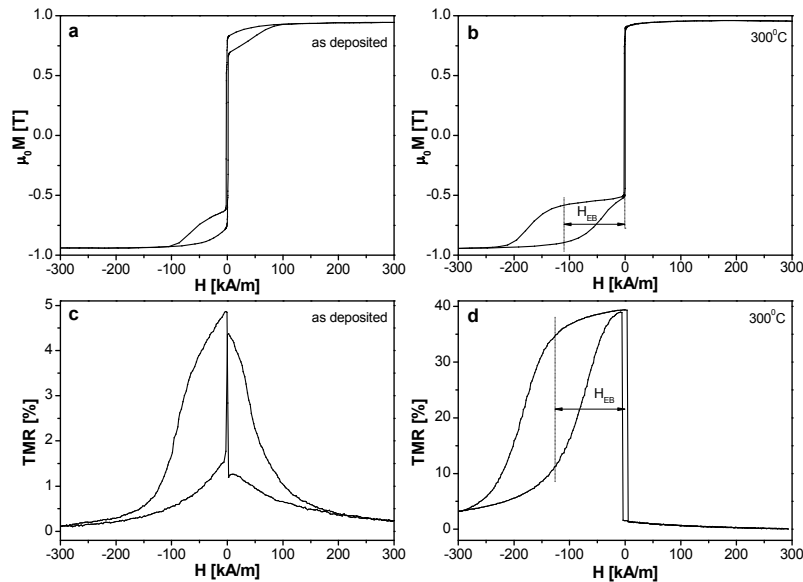

Fig. 5. Major loops for as deposited (left column) and annealed (right column) MTJ (with t =10 nm). Magnetization (a) and (b), TMR (c) and (d)

Fig. 5b and 5d. This is due to the increase of magnetic order of AF by field cooling, according to the model proposed by Tsunoda [13], where the AF layer is regarded as an aggregation of the AF grains with random distribution of the grain anisotropy axes. The mutual correlations between grain size, exchange biased and coercivity fields of annealed junctions are illustrated in Fig. 6. Accompanied by the change of grain size of $Ir_{25}Mn_{75}$, linear increase in exchange biased H_{EB} and coercivity H_{CP} fields of pinned layer $Co_{70}Fe_{30}$ was observed (Fig. 6).
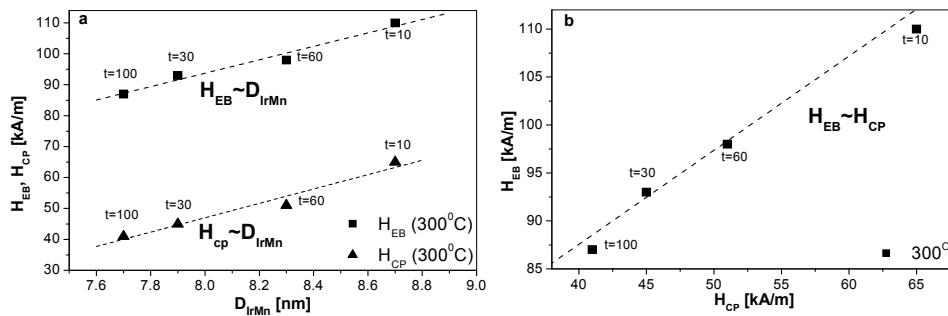

Fig. 6. The exchange biased field (H_{EB}) and the pinned layer coercivity field (H_{CP}) of annealed MTJ at $T = 300^{o}C$ (a) *vs.* grain size of IrMn. (b) The linear correlation between the exchange biased field and the pinned layer coercivity field of annealed MTJ at $T = 300^{o}C$.The dotted lines are fitted

Maximum value of $H_{EB} = 110$ kA/m (which corresponds to $J_{EB} = 3.6 \cdot 10^{-4}$ J/m^2) is for sample with $t = 10$ nm which grain size increase 24% between as deposited and annealed state.

3.3. Interlayer exchange coupling

Figure 7 shows the magnetization minor hysteresis loops in as deposited and annealed junctions. The as deposited samples are characterized by oblique hysteresis loops, large coercivity and slow switching while the annealed ones are characterized by rectangular hysteresis, fast switching and smaller coercivity. These changes in the shape of the hysteresis loops in relation to the magnetization process and domain structure, for as deposited and annealed junctions, are discussed in [16]. The minor loop of M(H) is always shifted in the direction indicating a ferromagnetic coupling between pinned (CoFe) and free (CoFe+NiFe) layers which is originated from the dipolar magnetic coupling (known as Nèel coupling or "orange peel" coupling). The decrease of interlayer coupling ($H_S = J/\mu_0 M_F t_F$) and coercivity (H_{CF}) fields of the free layer with increasing NiFe thickness (Fig. 8a and Table 2) in as-deposited and annealed samples, were observed. After annealing the interlayer coupling energy increases from $J = 0.75 \cdot 10^{-5}$ J/m^2 to $1.04 \cdot 10^{-5}$ J/m^2 whereas H_{CF} of free layer decreases (compare the empty and solid triangles in Fig. 8a). The variations of H_S and H_{CF} for as deposited and annealed junctions correlate linearly (Fig. 8b). The enhancement of interlayer coupling between pinned and free layers after thermal annealing indicates the correlated in-phase roughness of dipolar interacting interfaces – according to the model of columnar structure with conformal waviness proposed by Kools *et al.* [17] – due to the increase of crystallites size of NiFe. Discussed in our previous paper [18] the roughness amplitudes for
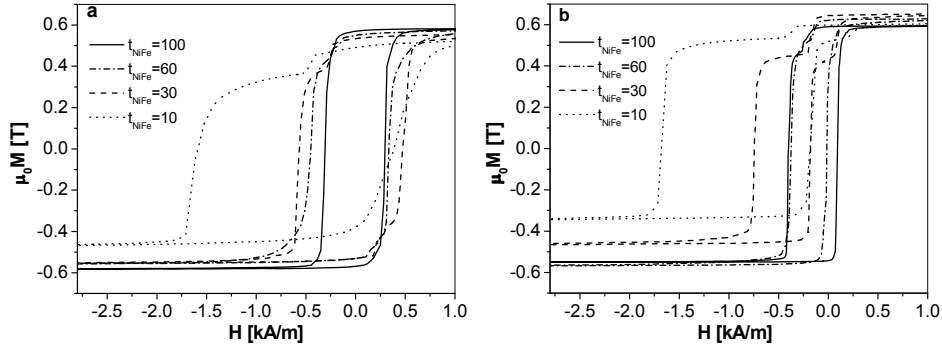
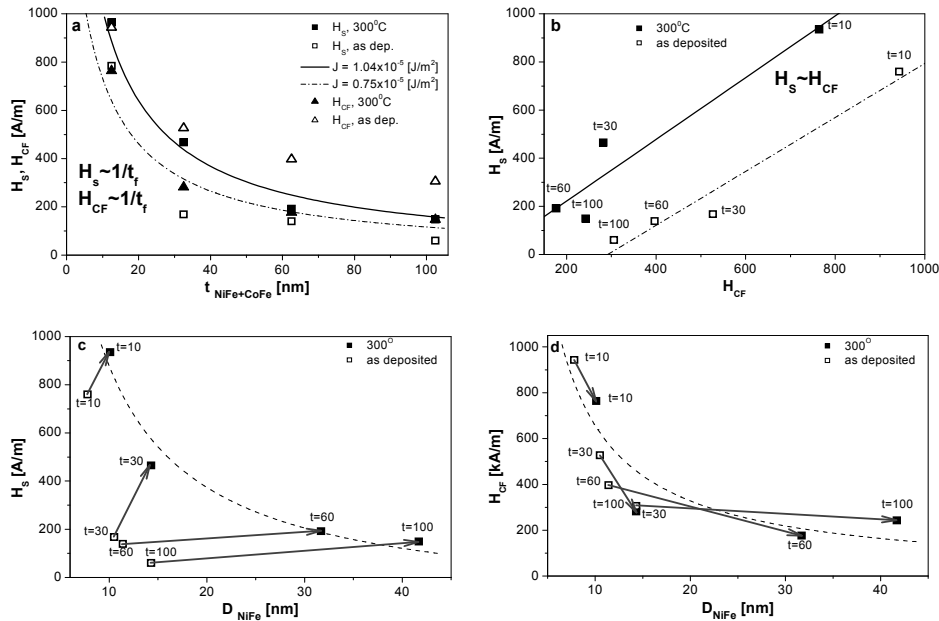Fig. 7. R-VSM minor loops (a) for as deposited and (b) annealed at 300°C MTJs

Fig. 8. (a) The interlayer coupling field and coercivity field for as deposited and annealed junctions *vs.* free layer thickness. (b) The linear correlation between interlayer coupling field and coercivity field of the free layer. (c) The interlayer coupling field *vs.* grain size of NiFe. (d) The coercivity field of the free layer *vs.* grain size of NiFe. The solid and dotted lines in (a) an (b) are fitted. The dashed lines in (c) and (d) are guides of eyes, representing reciprocal proportionality

similar system, determined by the atomic force microscope, for the surface of pinned and free layer were 6 ± 0.5 Å and 5 ± 0.5 Å, respectively, and are about two times higher than these obtained for non-textured layer stack [19]. From the plots for the changes of H_S and H_{CF} as a function of the crystallite size of NiFe (D_{NiFe}), we found that H_{CF} follows the $1/D_{NiFe}$

dependence (Fig. 8d, compare for the particular NiFe thickness the empty and solid squares), but that H_S for as deposited samples does not follow it (Fig. 8c). This contrast is owing to the remarkably small H_S against H_{CF} in as-deposited films as shown in Fig. 8b and indicates the difference of the lateral correlation length of the respective interlayer-coupling phenomenon. Taking into account that the pinned layer magnetization of as-deposited films makes domain structure in the film plane under the small field range, in which the free layer switches its magnetization (as shown in Fig. 5a), we can conclude that the lateral correlation length of H_S is longer than that of H_{CF}.

4. CONCLUSIONS

Complete and systematic XRD measurements indicate improvement of (111)-*fcc* texture of Cu, IrMn and NiFe planes, and enlarged crystallites size of IrMn after 300°C annealing, which leads to the increase of exchange biased and coercivity fields of the pinned layer. The large H_{EB} and H_{CP} are required for stable switching of MTJ. The enhancement of interlayer coupling energy, good remanence and coercive squareness, and softening of the free layer hysteresis loop is due to the increase of permalloy grains size after annealing treatment.

Acknowledgements

References

[1] J. Noguès and Ivan K. Schuller, J. Magn. Magn. Mat. **192**, 203 (1999).
[2] M. Takahashi and M. Tsunoda, J. Phys. D: Appl. Phys. **35,** 2365 (2002).
[3] A. E. Berkowitz and K. Takano, J. Magn. Magn. Mat. **200**, 552 (1999)
[4] M. Pakala, Y. Huai, G. Anderson, and L. Miloslavsky, J. Appl. Phys. **87**, 6653 (2000).
[5] K. Yagami, M. Tsunoda, and M. Takahashi, J. Appl. Phys. **89**, 6609 (2001).
[6] G. Anderson. Y. Huai, and L. Miloslavsky, J. Appl. Phys. **87**, 6989 (2000).
[7] J. van Driel, F.R. de Boer, K.-M. H. Lenssen, and R. Coehoorn, J. Appl. Phys. **88**, 975 (2000).
[8] H. Li, P.P Freitas, Z. Wang, J.B. Sousa, P. Gogol, and J. Chapman, J. Appl. Phys. **89**, 6904 (2001).
[9] K. Hoshino, R. Nakatani, H. Hoshiya, Y. Sugita, and S. Tsunashima, Jpn. J. Appl. Phys.**I35,** 607 (1996).
[10] R. Nakatani, H. Hoshiya, H. Hoshino, and Y. Sugita, J. Magn. Magn. Mat. **173**, 321 (1997).
[11] A. J. Devasahayam, P. J. Sides, and M. H. Kryder, J. Appl. Phys. **83**, 7216 (1998).
[12] M. Tsunoda, K. Nishikawa, S. Ogata, and M. Takahashi, Appl. Phys. Lett. **80**, 3135 (2002).
[13] M. Tsunoda and M. Takahashi, J. Magn. Magn. Mat. **239**, 149 (2002).
[14] M. Tsunoda and M. Takahashi, Journal of Magnetics (ed. Magnetic Korean Society) **7,** 80 (2002).
[15] J. Wrona, T. Stobiecki, M. Czapkiewicz, R. Rak, T. Ślęzak, J. Korecki, and C. G. Kim, J. Magn. Magn. Mat. **272-276** (3), 1629 (2004).
[16] M. Czapkiewicz, M. Żolądź, J. Wrona, P. Wiśniowski, R. Rak, T. Stobiecki, C. G. Kim, C.O. Kim, M. Tsunoda and M. Takahashi, phys. stat. sol. (b) **241 17**, 1477 (2004),.
[17] J. C. S. Kools, W. Kula, D. Mauri, and T. Lin, J. Appl. Phys. **85**, 4466 (1999).
[18] C. G. Kim, C.-O. Kim, Y. Hu, J. Kanak, T. Stobiecki, M. Tsunoda, and M. Takahashi, Materials Science **21** (1), 9 (2003).
[19] A. Thomas, *Preparation and characterization of magnetic single and double barrier junctions*, PhD thesis, University of Bielefeld (2003).